2019

A Comprehensive Case Report for the University of Montana Forensic Anthropology Laboratory Case #18-188

Elizabeth Rose Valentine

A COMPREHENSIVE CASE REPORT FOR THE UNIVERSITY OF MONTANA FORENSIC ANTHROPOLOGY LABORATORY CASE #18-188

By

ELIZABETH ROSE VALENTINE

BA, University of Wyoming, Laramie, Wyoming, 2018

Professional Paper

presented in partial fulfillment of the requirements
for the degree of

Master of Arts
in Anthropology, Forensics

The University of Montana
Missoula, MT

December 2019

Approved by:

Scott Whittenburg, Dean of The Graduate School
Graduate School

Randall Skelton, Chair
Anthropology

Kirsten Green-Mink
Anthropology

Tully Thibeau
Linguistics

Valentine, Elizabeth, M.A., Autumn 2019 Anthropology

A Comprehensive Case Report for the University of Montana Forensic Anthropology Laboratory Case #18-188

Committee Chair: Dr. Randall R. Skelton

This report consists of the skeletal remains, assessment of the minimum number of individuals, a biological profile analysis and a literature review on pathology analyses for forensic anthropology case reporting. The human remains are consistent with a MNI of one. The individual is likely an adult male of European ancestry with an estimated age range of 30 to 50 years at time of death. This individual has a probable forensic stature of 5’3’’ to 5’4’’. This individual may be identified by the burr hole or trepanation located on the frontal bone as there are likely medical records for this procedure.

Introduction

A forensic analysis was completed for case #18-188 to determine age, sex, ancestry, stature and dentition along with trauma and associated pathologies. Before biological profile analysis could be performed, several general observations are noted here.

A skeletal inventory was completed in order to assess the minimum number of individuals (MNI) for case #18-188. In addition to the MNI determination, the presence and condition of the skeletal remains was documented. The remains consist of completely skeletonized cranial and post-cranial elements in relatively good condition (Figure 1). The bones present include a complete crania and mandible. The following dentition are present: a right maxillary central incisor, a right maxillary lateral incisor, a right maxillary canine, a right maxillary first premolar, a right maxillary first molar, a left maxillary lateral incisor, a left maxillary canine, a left maxillary second premolar, a left maxillary first molar, a right mandibular central incisor, a right mandibular lateral incisor, a right mandibular first premolar, a right mandibular second premolar, a left mandibular central incisor, a left mandibular lateral incisor, a left mandibular canine, a left mandibular first premolar and a left mandibular third molar (Figure 13). In addition, the right clavicle, both scapula, humeri, ulnae, and radii are present. Furthermore, the sacrum, the left and right os coxae, both femora, both tibiae, and both fibulae are present. Lastly, 7 cervical vertebrae, 12 thoracic vertebrae, and 5 lumbar vertebrae are present along with 11 left ribs, 11 right ribs, and two unsided rib fragments. Based on the complete skeletal remains with no repeating elements, the MNI is determined to be 1.

While the centrum and neural arch are present for all vertebrae, there is damage to the spinous process of C-3, C-4, T-4, T-5 and T-6. There is transverse process damage to C-7, T-4, T-5, T-6, T-9, T-

10 and L-5. Vertebrae T-9 and T-10 appear to be the most damaged. This may be the result of pathology or trauma resulting from processing of this individual. A taphonomic section is not included in this analysis as the remains were processed at the Montana State Crime Lab prior to being received by the University of Montana Forensic Anthropology Laboratory (UMFAL).

Background

This is considered a modern forensic case as this individual was found on the West bank of the Clark Fork River in Missoula County on 19 July 2018. This individual is unidentified. An autopsy was performed on this individual indicating soft tissue was removed and the bones were processed at the Montana State Crime Lab.

Literature Review

On the frontal bone of the cranium, near the coronal suture, is a circular pathology measuring 12.25 by 15.28 millimeters (Figure 2). At first, this pathology is similar to a tuberculosis lesion. While the skull is an unusual area to be infected by tuberculosis, the cranial vault is the most common location for cranial tuberculosis (Roberts and Buikstra, 2019). Specifically, tuberculosis is most prevalent in the frontal bone of a cranium as opposed to other effected areas such as the cranial base and face (Roberts and Buikstra, 2019). While the lesion on the frontal bone of case # 18-188 is similar to the description of tuberculosis in that "the lesion is a round lytic focus of not more than 2 cm in diameter, with or without a 'moth-eaten' central sequestrum, terminating in complete perforation of the inner and outer tables," (Roberts and Buikstra, 2019: 382), tuberculosis is an unlikely diagnosis for this individual. In order for a tuberculosis lesion to appear on the cranium, this individual would have to exhibit secondary complex tuberculosis. This means the individual would have to present advance stages of tuberculosis evident on other skeletal elements such as the ribs, prior to tuberculosis being

evident in the cranium (Table 1). Thus, since no evidence of tuberculosis is present throughout the post-cranial skeleton, it is unlikely a singular lesion of tuberculosis would be present on the cranium, (Roberts and Buikstra, 2019). While the lesion on the frontal bone is unlikely to be the result of tuberculosis, it does resemble a syphilitic lesion.

Venereal syphilis in skeletal remains is classified as a tertiary stage or rather, the most advance stage. Of all tertiary bone lesions, 70% appear on the tibia, the bones surrounding the nasal cavity and on the skull, (Roberts and Buikstra, 2019). While this lesion is similar in appear to the characteristic "carries sicca" or "circular and rolled up inwards" appearance of syphilis, it again is an unlikely diagnosis for this individual. The lesion present on the frontal bone of the cranium exhibited in case # 18-188 is probably not the result of syphilis as there is no evidence of syphilis in the nasal and palatine bones, (Roberts and Buikstra, 2019). Since the lesion located on the frontal bone of this individual is not likely to be caused by tuberculosis or syphilis, a pathological explanation is not probable.

The probable cause of this lesion may be the result of trepanation. Trepanation is the "practice of drilling or scraping a hole into the skull's cranial vault to expose the brain's dura mater," (Gross, 2012) in order to alleviate pressure within the skull caused by brain injuries or infection. Trepanation has a long history as one of the world's oldest surgeries; it is believed that trepanation was first practiced among the prehistoric populations of Peru in the Early Intermediate Period, (Gross, 2012). Furthermore, it has been practiced in nearly every culture from ancient Greece and Rome, to cultures in Africa, Asia and the Pacific Islands (Gross, 2012). While trepanation was practiced in several parts of the world, it was performed for different reasons. In places such as South America, trepanation was performed with evidence of blunt force trauma, which suggests the practice of trepanation was used as a treatment. However in

places such as Western Europe, the surgery was performed to release evil spirits, insanity and epilepsy (Gross, 2012). Moreover, trepanation was successful, with a 50-70% success rate; this is evidenced by healing in the cranial vault. Not only was trepanation successful-but also, in many skeletal remains, roughly 33% had more than one trepanation in the crania, indicating that the procedure was performed more than once in the same patient (Gross. 2012).

While trepanation is traditionally acknowledged in an archaeological context, the medical procedure still has modern applications as well. In a modern context, trepanation is used for the relief of epidural and subdural hematomas (Han et al., 2009). This is caused by trauma to the brain resulting in bleeding between the skull and the dura or bleeding between the dura and the arachnoid (Han et al., 2009). Both conditions require surgical intervention called a burr hole trepanation to drain the bleeding and relieve pressure from the brain. The location and size of the burr hole is dependent on location and severity of the injury, but burr holes generally have specific locations on the frontal, parietal, temporal and middle meningeal artery (Figure 3), (Han et al., 2009). Modern burr holes also tend to be 3 by 3 centimeters due to the perforator or burr bit instrument utilized. Unlike their ancient predecessors, these burr holes are more likely to be perfectly circular.

Another modern example in which trepanation is utilized is that of cochlear implants. A cochlear implant is a small medical device with internal and external attachments. The internal attachment is a small electronic device that electronically stimulates the cochlear nerve or the nerve used for hearing (James et al, 2004). The actual trepanation for this device is distinctive as it is always placed on the temporal bone near the mastoid process of the cranium. Furthermore, this form of trepanation will exhibit extensive healing throughout the lifetime of the receiver (James et al, 2004). Overall, it is unlikely that the trepanation on the frontal bone of the

individual for case #18-188 is caused by a cochlear implant due to the location of the exhibited lesion. It is however likely that this circular trauma is the result of a premortem and modern medical surgery. Again, the circular lesion on the frontal bone of this individual is almost perfectly circular and fits within the 3 cm by 3 cm criteria of a burr drill hole. It also resembles the location of a burr hole trepanation on the frontal bone of a cranium as illustrated in Figure 3.

Materials and Methods

To perform a forensic assessment for case #18-188, several methods were utilized to achieve estimations of age, sex, ancestry, stature, pathology and trauma. For aging of the individual, methods relating to the cranial sutures, the pubic symphyseal surface, and the auricular surface were employed. An age assessment using cranial suture sites was analyzed using the Meindl and Lovejoy (1985) method (Buikstra and Ubelaker, 1994). First, the vault sites to include the midlambdoid, lambda, obelion, anterior sagittal and bregma were used to create a composite score which was then associated with an "S" designation or subsequent age phase (Buikstra and Ubelaker, 1994). Next, a composite score was created for the following lateral-anterior sites: pterion, midcoronal, sphenofrontal, inferior sphenotemporal and superior sphenotemporal. This composite score was similarly associated with an "S" designation to create an overall age estimation (Figure 4).

Furthermore, the pubic symphyseal surface was assessed using the Todd (1920) and Suchey-Brooks (1990) method. The Todd pubic symphysis scoring system (Buikstra and Ubelaker, 1994) used ten phases and their corresponding descriptions to determine age in an individual while the Suchey-Brooks pubic symphysis scoring system used similar descriptions to

translate age into six phases. The pubic symphyseal surface of the left innominate from case #18-188 was categorized into one of these phases using the respective scoring system.

Lastly, age estimation was determined for case #18-188 using the auricular surface of the ilium. Specifically, the superior demiface, inferior demiface, rectroauricular area, the preauricular surface and the apex of the auricular surface was analyzed using the Lovejoy (1985) method and the Buckberry and Chamberlain (2002) method. The scoring system for the Lovejoy (1985) method includes matching the auricular surface to a description of corresponding phases and subsequent ages. Moreover, a new method of analysis was used in determining age from the articular surface of the ilium by Buckberry and Chamberlain (2002). This system is a revised method of the Lovejoy aging system utilizing the same skeletal feature, but differs in that the age related stages for different features of the articular surface are graded independently to provide a composite score which is then correlated to the estimates for age-at-death as established by Lovejoy (Buckberry and Chamberlain, 2002).

First, a composite score is recorded for transverse organization with scores ranging from 1-5. A score of 1 dictates that 90% or more of the auricular surface is transversely organized while a score of 5 denotes that no transverse organization is present. Next, surface texture is scored from 1-5 with a score of 1 being 90% or more of the auricular surface is finely granular and a score of 5 being 50% or more of the surface is occupied by dense bone. Furthermore, microporosity and macroporosity is scored from 1-3 with 1 meaning no micro or macroporosity is present on the demiface and a 3 meaning micro or macroporosity is present on both demifaces. Lastly, following suit is the scoring system for apical changes which ranges from 1-3. A score of 1 illustrates that the apex is sharp and distinct and the auricular surface may be slightly raised relative to adjacent bone surface while a score of 3 illustrates that the apex irregularly occurs in

contours of auricular surface and the shape of the apex is no longer a smooth arc (Buckberry and Chamberlain, 2002). These individual scores are lastly added together to create a composite score which is then translated to the Lovejoy aging system; a composite score of 5-6 translates to stage I while a composite score of 17-19 correlates to stage VII.

Sex

For sexing of the individual, sex estimation using non-metric features of the pelvis, non-metric features of the skull, sexing of the femur and the humerus using post-cranial measurements and visual methods for sexing of the os pubis were utilized. Sex estimation was analyzed using non-metric features of the pelvis according to the Klales (2012) method. This method uses a logistic regression equation as well as linear discriminant functions to determine sex by scoring the following features of the pelvis: the sub-pubic concavity, the medial ischiopubic ramus and the ventral arc. Each feature is given a score from 1 to 5 with 1 representing a more feminine pelvis and 5 being a more masculine pelvis. Furthermore, sex estimation was analyzed using non-metric features of the skull according to the Walker (2008) method. This method also uses a logistic regression equation to determine sex based on scoring of the following cranial characteristics: the nuchal crest, the mastoid process, the supraorbital margin, the glabella and the mental eminence. Again, each characteristic is rated from 1 to 5 with 1 being more gracile or feminine features and 5 being more robust or masculine features.

Moreover, sexing of the femur and the humerus using post-cranial measurements and visual methods of the os pubis were utilized in assessing sex for individual #18-188. Post-cranial measurements include 44 measurements of 11 elements to the nearest millimeter. All measurements utilized the left side. These measurements were used with FORDISC 3.0 (Jantz

and Ousley, 2005) to analyze sex. Also post-cranial measurements were used to sex an individual using the femur; the following measurements are utilized: maximum diameter of the femoral head (Stewart, 1979), the circumference of the mid-shaft (Black, 1978), and the maximum length of the femur (Thieme, 1957). This method estimates that a male individual will have a maximum diameter of the femoral head over 47.5 millimeters, a circumference of the femoral mid-shaft greater than 81 millimeters, and a maximum length of the femur greater than 455 millimeters. Measurements of a female individual will be less than 42.5 millimeters for the maximum diameter of the femoral head, less than 81 millimeters for the mid-shaft circumference, and less than 415 millimeters for the maximum length for the femur. Sexing of the humerus uses the following measurements: the vertical diameter of the humeral head (Stewart, 1979) and the maximum length of the humerus (Thieme, 1957). For a male individual, measurements of the vertical diameter of the humeral head are greater than 47 millimeters and a maximum humeral length is greater than 340 millimeters. A female individual will have a vertical diameter of the humeral head less than 43 millimeters and a maximum length of the humerus less than 300 millimeters.

Lastly, a sex determination was assessed using visual methods of the os pubis according to Phenice (1969); Buikstra and Ubelaker (1994). This method consists of using visual assessments in rating the ventral arc, the subpubic concavity and the ischiopubic ramus ridge from 1 to 3; the greater sciatic notch from 1-5 and the preauricular sulcus from 0-4.

Ancestry

For estimating ancestry of the individual, cranial measurements and FORDISC 3.0, macromorphoscopics, nonmetric traits assessment and measurements of the scapula were used.

First, ancestry was determined using 34 measurements of the crania. These measurements were taken with a spreading and sliding caliper and further recorded to the nearest millimeter. When applicable, measurements were taken on the left side. Furthermore, these measurements were used with FORDISC 3.0 under modern populations which results in a two group discriminant function test. This method classifies the individual into an ancestry based on probabilities and distance from other groups. All available ancestries were utilized in FORDISC 3.0 for this test until two ancestries could be narrowed down by reaching a posterior probability close to 1.0. These ancestries were European and African American.

Next, ancestry was assessed using macromorphoscopics and the optimized summed scored attributes (OSSA) scoring sheet. This method uses the following characteristics to create a predicted ancestry: anterior nasal spine, nasal aperture width, inferior nasal aperture, nasal bone contour, interorbital breadth and post-bregmatic depression. Each characteristic is thus given an appropriate score. The anterior nasal spine is scored from 1 to 3. A score of 1 means slight, 2 means intermediate and 3 means marked. The nasal aperture width is similarly scored from 1 to 3. A score of 1 denotes a narrow aperture width, a score of 2 denotes a medium width and a score of 3 denotes broad aperture width. The inferior nasal aperture is scored from 1 to 5. A score of 1 indicated the nasal aperture has a pronounced slope while a score of 2 is a moderate slope. A score of 3 indicates the nasal aperture is straight and a score of 4 indicates the nasal aperture has a partial sill while a score of 5 indicates the inferior nasal aperture has a sill. The nasal bone contour is scored from 0-4. A score of 0 illustrates a low or round nasal bone contour while a score of 1 illustrates an oval shape, 2 illustrates a steep and marked plateau, 3 illustrates a steep and narrow plateau and lastly a score of 4 illustrates a triangular nasal bone contour. The interorbital breadth is scored from 1 to 3. A score of 1 means the interorbital breadth is narrow

while a score of 2 means the interorbital breadth is intermediate and a score of 3 means the interorbital breadth is wide. The last scored characteristic is the post-bregmatic depression. The post bregmatic depression is either given a score of 0 or 1. A score of 0 means there is no post-bregmatic depression present and alternatively, a score of 1 means a post-bregmatic depression is present. This method results in an overall summed score and a summed compressed score in order to give a predicted ancestry.

Furthermore, nonmetric traits assessment was used in determining ancestry. For this method, nonmetric traits in determining ancestry based on the cranium Rhine (1990) and Gill (1995) were used along with primary nonmetric traits assessment by Buikstra and Ubelaker (1994). For the Rhine and Gill methods, the following elements or characteristics of the crania were analyzed: the incisors, zygomatics, prognathism, palate, cranial sutures, nasal spine, chin, ascending ramus, palatine suture, zygomatic tubercle, incisor rotation, nasal profile, sagittal arch, wormian bones, nasals, nasal aperture, zygomaticomaxillary suture, dentition, nasal sill, nasion, cranial vault, mandible, inion hook and post-bregmatic depression. The other method by Buikstra and Ubelaker used the following elements or characteristics in analyzing ancestry: the metopic suture, supraorbital notch, supraorbital foramen, infraorbital suture, multiple infraorbital foramina, zygomatico-facial foramina, parietal foramen, sutural bones, inca bone, condylar canal, divided hypoglossal canal, flexure of the superior sagittal sulcus, foramen ovale incomplete, foramen spinosum incomplete, pterygo-spinous bridge, pterygo-alar bridge, tympanic dehiscence, auditory exostosis, mastoid foramen, mental foramen, mandibular torus, mylohyoid bridge, atlas bridging and septal aperture.

The last method utilized in determining ancestry for case #18-188 involved measurements of the scapula. This method (Krogman 1962) used a scapular index to predict

ancestry. The scapular index is equal to the maximum breadth of the scapula multiplied by 100 and divided by the maximum length of the scapula. The scapular index is then compared to a range of scores from known population data. The scapular index correlates to a range of averages within sex and ancestry.

Stature

For estimating stature, methods by Trotter (1970), FORDISC 3.0 and a short regression formula (Duyar et. al, 2005) were utilized. For the Trotter (1970) stature estimation, an ancestry specific formula is used. The formula uses the femur maximum length, the fibula maximum length and the humerus maximum length to produce a point estimate, a prediction interval and a predicted stature range in inches. Moreover, in FORDISC 3.0 these measurements are used to create a predicted forensic stature. Again, stature is calculated by ancestry and a 90% predication interval or confidence probability of the estimation. This method uses a population of 20th century forensic statistics.

Forensic stature was further analyzed using a new method of stature estimation using a short regression formula, (Duyar et. al, 2005). This formula is based on different categories of stature groups: short, medium, and tall. For case #18-188, the ulna short regression equation, tibia short regression equation as well as ulna and tibia short regression equation was used. The ulna short regression equation is 1313.48 plus 1.133 times the maximum length of the ulna in millimeters equals stature. The tibia short regression equation is 753.89 plus 2.421 times the maximum length of the tibia in millimeters equals stature. Lastly, the ulna and tibia short regression equation is 728.82 plus 0.255 times the maximum length of the ulna in millimeters

plus 2.307 times the maximum length of the tibia in millimeters equals stature. Overall, these three stature estimations are averaged to give overall forensic stature estimation.

Dentition

The dentition for this case was analyzed using a dental inventory visual recording form of permanent dentition taken from Standards (Buikstra and Ubelaker, 1994) as well as a antemortem dental modification recording form, and a dental inventory recording form of development, wear and pathology for permanent teeth. Furthermore, case #18-188 received dental x-rays and analysis from the Curry Dental Health Center at the University of Montana.

The dental inventory visual recording form of permanent dentition "assigns numbers 1-32 to the permanent dentition, beginning with the maxillary right third molar (1), continuing to the mandibular right third molar (32)," (Buikstra and Ubelaker, 1994: 47). On this recording form, not only the absence or presence of dentition is noted but conditions such as fillings, carious lesions and calculus are indicated as well. For the premortem dental modifications recording form, modifications such as filings, drillings with or without inlays, dental restorations and appliances, dental wear associated with artifact use or production and tooth ablation are categorized.

Moreover, the dental inventory recording form for development, wear and pathology are organized into categories such as tooth presence, development, wear, caries, abscess and calculus. For the tooth presence category, teeth are coded on a scale of 1-8. A score of 1 means the tooth is present but not in occlusion, a score of 2 means the tooth is present-the development is completed and in occlusion, a score of 3 means the tooth is missing with no associated alveolar bone, a score of 4 means the tooth is missing with alveolus resorbing or fully resorbed indicating

the tooth is a premortem loss, a score of 5 means the tooth is missing with no alveolar resorption indicating the tooth is a postmortem loss, a score of 6 means the tooth is missing as a congenital absence, a score of 7 means the tooth is present but damage renders measurement impossible though other observations are recorded and a score of 8 means the tooth is present but unobservable.

The scoring system for the wear is assigned to 8 stages. These stages are specific to the incisors and canine, the premolars and the molars. These descriptions can be found in Figure 5 and Figure 6 of the Appendix. The scoring system for caries is on a scale of 0 to 7. A score of 0 indicates that no lesion is present. A score of 1 indicates that there are carious lesions on the occlusal surface. A score of 2 indicates that there are carious lesions on the interproximal surfaces while a score of 3 indicates that there are caries on the smooth surfaces. A score of 4 indicates that there are cervical caries present while a score of 5 indicates that there are root caries below the CEJ (cervicoenamel junction). A score of 5 indicates that there are large caries that have destroyed so much of the tooth that they cannot be assigned a surface of origin and lastly a score of 7 indicates that there is noncarious pulp exposure on the tooth. Lastly, this method includes a scoring system for calculus. Calculus is reported as 1 meaning no calculus is present, 1 meaning a small amount of calculus is present, 2 meaning a moderate amount of calculus is present, 3 meaning a large amount of calculus is present and 9 meaning calculus is unobservable. This method furthermore has a scoring system for abscesses but it is not described here as it was not observed in this individual.

Pathology & Trauma

To analyze pathology and trauma for case #18-188, the following references were utilized: Ortner's Identification of Pathological Conditions in the Human Skeletal Remains (Buikstra, 2019), The Human Bone Manual (White and Folkens, 2005) and Standards for Data Collection from Human Skeletal Remains (Buikstra and Ubelaker, 1994). Abnormalities for this individual were noted and then referenced to these materials to aid in identifying pathologies for this case.

Results

In regards to the cranial suture (Meindl and Lovejoy, 1985; Buikstra and Ubelaker, 1994) age assessment for case #18-188, the vault sites resulted in a 10 composite score which is equal to an "S" phase of S3. The estimation based on the vault sites indicates that this individual was between the ages of 27-44 with a mean age of 38 at time of death. The lateral anterior sites resulted in a composite score of 14 and an "S" phase of S7. The S7 phase indicates that this individual was between the ages of 47-60 with a mean age of 56 at time of death.

The age assessment utilizing the pubic symphysis for the Todd (1920) method resulted in a score of 5 for the left innominate and 5 for the right innominate. This results in an age estimate of 27-30 years old at time of death. The Suchey-Brooks (1990) method resulted in a score of 4 for the left innominate and 4 for the right innominate. This produces an estimate of 35 years of age at time of death. Furthermore, the auricular surface resulted in a score of 3 for the left innominate and 4 for the right innominate. This method estimates the individual to be 30-39 years old at time of death.

Lastly, the age estimate utilizing the revised method from the auricular surface of the ilium by Buckberry and Chamberlain (2002) produced the following results: the transverse organization was given a score of 3, the surface texture was given a score of 3, microporosity was given a score of 1, macroporosity was given a score of 1 and apical changes was given a score of 2. This cumulated in a composite score of 10 which resulted in an age stage of 3. This creates an age estimation of 30-34 years old at time of death for this individual.

Sex

The sex estimation using non-metric features of the pelvis resulted in a score of 4 for the subpubic concavity, a score of 3 for the medial ischiopubic ramus, and a score of 4 for the ventral arc. The logistic regression equation estimates this individual to be a probable male with a 93% confidence probability (Figure 7). Furthermore, the sex estimation utilizing the non-metric features of the skull resulted in a score of 4 for the nuchal crest, a score of 4 for the mastoid process, a score of 2 for the supraorbital margin, a score of 3 for the glabella and a score of 4 for the mental eminence. The logistic regression equation also concludes this individual to be a probable male with a 97% percent confidence probability (Figure 8). Sexing using measurements of the femur resulted in 44.23 millimeters for the maximum diameter of the femoral head, 96 millimeters for the circumference of the mid-shaft, and 438 millimeters for the maximum length of the femur. The results of sexing using measurements of the humerus were 46.82 millimeters for the vertical diameter of the humeral head and 307 millimeters for the maximum length of the humerus.

Lastly, the sex determination using visual methods of the os pubis according to Phenice (1969); Buikstra and Ubelaker (1994) resulted in the same score for both the right and the left

innominate. The ventral arc was given a score of 3, the subpubic concavity was given a score of 3, the ischiopubic ramus ridge was given a score of 3 and the greater sciatic notch was given a score of 4. The preauricular surface was not given a score as it was absent in this individual. Overall, these results conclude the individual was a probable male.

Ancestry

The results of using cranial measurements and FORDISC 3.0 to predict ancestry estimated the individual to be of European descent. The ancestry results did not include measurements for the palate breath, the mastoid height, the mandibular length or the orbital breath. FORDISC determined using a two group discriminant function test that the individual was a white male with a 99% posterior probability, a typicality F of 8.9%, a chi typicality of 0.0% and a typicality R of 2.6% (Figure 9). Moreover, the results of the macromorphoscopics (Figure 10) and OSSA scoring sheet (Figure 11) also concluded the individual was of probable European ancestry. The score for the anterior nasal spine was 3, the score for the nasal aperture width was 1, the inferior nasal aperture was given a score of 5, the nasal bone contour was given a score of 2, the interorbital breath was given a score of 3 and the post-bregmatic depression was given a score of 0. This produced a sum score of 5 and subsequently a European predicted ancestry.

Next, the following characteristics of the nonmetric traits assessment based on the cranium were considered to be of European ancestry: blade formed incisors, limited prognathism, parabolic palate, long-projecting nasal spine, and a present inion hook. The following characteristics were considered to be of African American ancestry: low flat nasals, wide nasal aperture, large molars and low cranial vault. Lastly, the following characteristics

were considered to be of Native American ancestry: straight palatine suture, concave-convex nasal profile, and angled zygomaticomaxillary suture. The zygomatics, chin, ascending ramus, zygomatic tubercle, incisor rotation, sagittal arch, wormian bones, nasal sill, nasion, mandible and post-bregmatic depression was not assessed. Lastly, measurements of the scapula produced a scapular index of 75.08 indicating an African American ancestry.

Stature

The results of the Trotter (1970) method for European ancestry estimate the height of the individual to be between 62-65 inches or 5'2''- 5'5''. The point estimate using the maximum length of the femur was 64.28 inches with a prediction interval of 2.8%. The predicted stature range was 62.99 to 65.57 inches in height. The point estimate for the maximum length of the fibula was 64.24 inches. The prediction interval was not calculated by Todd (1920). The predicted stature range was 62.94 to 65.54 inches in height. Lastly, the point estimate for European ancestry using the maximum length of the humerus was 63.87 inches with a prediction interval of 3.3%. The predicted stature range was 62.28 to 65.47 inches. Although the ancestry of this individual is likely European, stature estimates were calculated for African American ancestry as well for comparison. The point estimate using the maximum length of the femur was 63.25 inches with a prediction interval of 4.0%. The predicted stature range was 61.70 to 64.80 inches in height. The point estimate using the maximum length of the fibula was 63.12 inches. The prediction interval was not calculated by Todd (1920) however, the predicted stature range was 61.52 to 64.73 inches in height. Lastly, the point estimate using the maximum length of the humerus was 62.70 inches with a prediction interval of 4.4%. The predicted stature range was 60.95 to 64.44 inches in height.

When the post-cranial measurements were used with FORDISC 3.0 using European male ancestry, the results concluded that predicted forensic stature for the individual was between 62.4 to 68.9 inches with a confidence interval of 90% (Figure 12). Lastly, the short regression formula for the ulna resulted in an estimate of 62.99 inches or an individual which is 5'3'' tall. The short regression formula for the tibia resulted in an estimate of 63.99 inches or an individual which is 5'4'' inches tall. The ulna and tibia short regression formula resulted in an estimate of 63.84 inches or 5'3'' tall.

Dentition

The results for the dental inventory visual recording form for permanent dentition include the presence of the following dentition in abbreviation: RI^1, RI^2, RC^1, RP^1, RM^1, LI^2, LC^1, LP^2, LM^1, RI_1, RI_2, RC_1, RP_1, RM_3, LI_1, LI_2, LC_1, LP_1 and LP_2. Additionally, the results of the premortem dental modifications recording form indicated that the individual had aesthetic modification in the form of a filling on the left and right maxillary first premolar. The left and right second and third molars have been removed possibly through tooth ablation. The mandibular left first, second and third molars may have also been removed via tooth ablation along with the right first and second molars.

The results of the dental inventory recording form for development, wear and pathology for permanent teeth are as follows: the tooth presence for RM^3 was given a score of 4, RM^2 was given a score of 4, RM^1 was given a score of 2, RP^2 was given a score of 4, RP^1 was given a score of 7, RC^1 was given a score of 7, RI^2 was given a score of 2 and RI^1 was given a score of 2. The score of 8 was assigned to LI^1, a score of 2 was assigned to LI^2, a score of 2 was assigned to LC^1, a score of 4 was assigned to LP^1, a score of 2 was assigned to LP^2, a score of 2 was

assigned to LM^1, a score of 4 was assigned to LM^2, and a score of 4 was assigned to LM^3. LM_3 LM_2 and LM_1 were given a score of 4, LP_2, LP_1, LC_1, LI_1 and LI_2 were given a score of 2. RI_1, RI_2, RC_1, and RP_1 were given a score of 2 while RP_2, RM_1, and RM_2 were given a score of 4. RM_3 was given a score of 7.

For wear, RM^3 was given a score of 0, RM^2 was given a score of 0, RM^1 was given a score of 3 for each cusp, RP^2 was given a score of 0, RP^1 was given a score of 7, RC^1 was given a score of 7, RI^2 was given a score of 6 and RI^1 was given a score of 5. The score of 8 was assigned to LI^1, a score of 3 was assigned to LI^2, a score of 5 was assigned to LC^1, a score of 0 was assigned to LP^1, a score of 3 was assigned to LP^2, a score of 3 was assigned to each cusp for LM^1, a score of 0 was assigned to LM^2, and a score of 0 was assigned to LM^3. LM_3 LM_2 and LM_1 were given a score of 0, LP_2 was given a score of 6, LP_1 was given a score of 7, LC_1 was given a score of 3, and LI1 and LI_2 were given a score of 4. RI_1 and RI_2 were given a score of 4, RC_1, and RP_1 were given a score of 3 while RP_2, RM_1, and RM_2 were given a score of 0. RM_3 was given a score of 10.

For the caries, RM^3 was given a score of 0, RM^2 was given a score of 0, RM^1 was given a score of 1, RP^2 was given a score of 0, RP^1 was given a score of 6, RC^1 was given a score of 6, RI^2 was given a score of 5 and RI^1 was given a score of 4. The score of 6 was assigned to LI^1, a score of 5 was assigned to LI^2, a score of 5 was assigned to LC^1, a score of 0 was assigned to LP^1, a score of 2 was assigned to LP^2, a score of 1 was assigned to LM^1, a score of 0 was assigned to LM^2, and a score of 0 was assigned to LM^3. LM_3 LM_2 and LM_1 were given a score of 0, LP_2 was given a score of 5, LP_1 was given a score of 4, and LC_1, LI_1 and LI_2 were given a score of 0. RI_1, RI_2, RC_1 were given a score of 0, and RP_1 were given a score of 5 while RP_2, RM_1, and RM_2 were given a score of 0. RM_3 was given a score of 6.

Lastly for calculus, RM^3 was given a score of 0, RM^2 was given a score of 0, RM^1 was given a score of 3, RP^2 was given a score of 0, RP^1 was given a score of 9, RC^1 was given a score of 9, RI^2 was given a score of 9 and RI^1 was given a score of 2. The score of 9 was assigned to LI^1, a score of 3 was assigned to LI^2, a score of 3 was assigned to LC^1, a score of 0 was assigned to LP^1, a score of 3 was assigned to LP^2, a score of 3 was assigned to LM^1, a score of 0 was assigned to LM^2, and a score of 0 was assigned to LM^3. LM_3 LM_2 and LM_1 were given a score of 0, LP_2, LP_1, LC_1, LI_1 and LI_2 were given a score of 3. RI_1, RI_2, RC_1, and RP_1 were given a score of 3 while RP_2, RM_1, and RM_2 were given a score of 0. RM_3 was given a score of 9.

The results of the dental x-rays and analysis can be seen in the Appendix as Figure 13-24. These results were not used to assess age in this individual but rather to evaluate the extent of dental care this individual has received. These results may potentially provide a positive identification of this individual compared with antemortem dental records.

Pathology & Trauma

Analysis for pathology includes a possible burr hole or trepanation on the left side of the frontal bone measuring 12.25 x 15.28 mm. There is osteoporosis on the inferior side of the left clavicle (Figure 25) and the inferior side of the right clavicle (Figure 26). There is osteoporosis, as described as an increased porosity of bone (White & Folkens, 2005) on the anteroinferior and posterosuperior left side of the sacrum (Figure 27 & 28). There are osteophytes, as described as a small and abnormal bony growth (White & Folkens, 2005) on the iliac crest (Figure 29) and ischial tuberosity of the left os coxae (Figure 30). The right os coxa has osteophytes on the preauricular surface (Figure 31), the iliac crest (Figure 32) and the ischial tuberosity (Figure 33) and osteoporosis on the ischial spine (Figure 34) and the auricular surface (Figure 35).

Furthermore, there are osteophytes on the spinal process of C-2 (Figure 36) along with osteoporosis on C-3 and C-4 (Figure 37) as well as on T-4, T-5, T-6, T-7, T-8, T-9 and T-10 (Figure 38 & 39).

There is healed trauma to the left of the glabella and above the left eye orbit measuring 25.76 by 17.09 mm (Figure 40). There is a postmortem cut to the sternal end of the left clavicle (Figure 41) and there is postmortem drilling on the left tibia on the anterior proximal side measuring 41.75 mm apart (Figure 42).

Discussion

With several methods employed to assess age in case #18-188, the conclusion can be made that this individual was likely between the ages of 30-50 years at time of death. While this individual is categorized as a middle adult, it was difficult to assess age due to the osteophytes near and on the auricular surface. Moreover, the manubrium was not fused to the sternum which further complicated age determination and the autopsy cut may have affected the cranial suture closure analysis. Age was further complicated with the extreme condition of the teeth exhibited in this individual. While determining age for this individual was difficult, the revised method for age estimation from the auricular surface of the ilium was the most accurate method in assessing age. This is due to the detailed descriptions it provides in determining characteristics of the auricular surface; the descriptions delineate exactly what microporosity, macroporosity and transverse organization should look like by every 10%. Furthermore, this method is useful in that it rates the retroauricular surface, inferior demiface, preauricular sulcus, apex and superior demiface separately. This creates a composite score which is easier to translate to the Todd (1920) method for aging using the auricular surface.

While methods such as cranial suture closure, pubic symphyseal surface and the auricular surface of the ilium were analyzed, other methods such as epiphyseal closure, sternal rib end and tooth eruption were not employed in assessing age for case #18-188. Methods involving epiphyseal closure (Buikstra and Ubelaker, 1994) and tooth eruption (Scott, 1979) were not analyzed in case #18-188 as this individual is not a subadult. The sternal rib end method was not analyzed in assessing age for this individual as determining the fourth rib is difficult to identify.

Sex

Based on the os coxae morphology, this individual is a probable male. The most obvious characteristics include a lack of subpubic concavity, a broad medial surface and a narrow greater sciatic notch. Based on the skull, this individual is most likely male as well. While this individual has sharp supraorbital margins, this individual has a glabella, nuchal crest and mental eminence most characteristic of a male. Due to the measurements of the femur, the maximum diameter of the femoral head concluded indeterminate sex estimation, the circumference of the mid-shaft concludes a male estimation and the maximum length of the femur indicates this individual is of indeterminate sex. The vertical diameter and the maximum length of the humerus also indicate this individual is of indeterminate sex. This method resulted in an indeterminate sex determination though the measurements of this individual were greater than the female estimations. These results may be influenced by the size or short stature of this individual. Overall, the assessments utilized for sex determination in case #18-188 classifies this individual as a probable male. These methods are easy to employ and interpret, increasing confidence in these results.

Ancestry

Ancestry is usually difficult to determine in an individual with complete certainty. This is due to populations being the result of globalization and population admixture, which leads to an issue of representation of standards. Populations that were used to develop the standards within FORDISC 3.0 may not actually be representative of the individual analyzed for this case due to background and distance in time. There are furthermore issues with the sample size of databases such as FORDISC 3.0 and even with a high posterior probability result in the two-group discriminant function test; the low typicality results suggest that even a high probable determination is wrong. The typicality results from FORDISC 3.0 suggest the ancestry estimation may be incorrect as only 0-2.6% of European males sampled actually resembles the individual from case #18-188. Overall, there are issues with FORDISC 3.0 primarily with identifying individuals with mixed ancestry. With these limitations being understood, the ancestry of this individual is likely European.

While the FORDISC 3.0 results may not classify this individual as of European ancestry, the most accurate methods used to obtain this result were the cranial macromorphoscopics. The visual assessments conclude this individual is likely European, primarily due to the nasal aperture. Other methods produced mixed results, however. The nonmetric traits in determining ancestry based on the cranium predicted an almost even number of characteristics belonging to Native American, African American and European categories. Yet, the most common characteristic was still of European ancestry. The last method, ancestry determination using measurements of the scapula (Krugman, 1962), was the only result to predict an African American ancestry. However, this method is the most outdated and least utilized for determining

ancestry within the Forensic Anthropology field. Though the results for ancestry varied, based on the macromorphoscopics results, this individual is of likely European ancestry.

Stature

The Trotter 1970 method concludes that this individual was likely between 5’3’’ and 5’4’’ tall at time of death. This estimation fits well within the predicted forensic stature of 5’2’’ to 5’8’’ given by FORDISC 3.0. Lastly, the new method of stature estimation (Duyar, 2005) also estimates this individual was likely between 5’3’’ and 5’4’’ tall at time of death. Since all these methods conclude the same stature estimation, it is likely this individual was between 5’3’’-5’4’’ tall at time of death however there are limitations for ancestry specific stature estimates which may make these results less accurate. The new method of stature estimation was useful in adding additional testing methods for stature as this method has the least amount of methods applicable to forensic anthropology. However, this method is only relative when applied to cases with individuals who are either shorter or taller than the standard curve. Thus it is dependent on the results of other methods.

Dentition

The results conclude that this individual has an extreme amount of wear, caries and calculus affecting the teeth. It is unclear whether the left and right maxillary and mandibular molars were removed via tooth ablation or lost due to poor dental health. Many of the absent teeth such as the molars and the maxillary left first premolar have been healed over suggesting these teeth were lost significantly prior to time of death. The dental x-rays completed by the Curry Health Center at the University of Montana indicate that more dental work was completed

than visible to the naked eye which may aid in providing a positive identification of this individual.

Pathology & Trauma

The osteoporosis and osteophytes exhibited indicate that this individual was physically active during their lifetime, especially given the 30-50 years of age estimation. The presence of these pathologies furthermore may have obscured the age range estimation- making this individual appear older. Additionally, the processing for case #18-188 may have exacerbated the osteoporosis displayed throughout the skeletal remains. Lastly, the burr hole or trepanation located on the frontal bone may be used to identify this individual as there should be medical records for this procedure. The trauma on the sternal end of the left clavicle and the drill holes on the left tibia exhibited for case #18-188 is postmortem- likely the result of processing these skeletal remains.

Conclusion

A forensic analysis was completed for case #18-188 to determine age, sex, ancestry, stature and dentition along with trauma and associated pathologies. Several methods were employed to conclude that the human remains are consistent with a MNI of one. The individual is likely an adult male of European ancestry with an estimated age range of 30 to 50 years at time of death. This individual has a probable forensic stature of 5’3’’ to 5’4’’. This individual may be identified by the burr hole or trepanation located on the frontal bone as there are likely medical records for this procedure.

Appendix

Table 1: This table illustrates the location of bone lesions in skeletal tuberculosis by order of decreasing frequency (Roberts and Buikstra 2019, 382).

TABLE 11.2 Locations of Bone Lesions in Skeletal Tuberculosis Listed in Order of Decreasing Frequency

Location	No. of Instances
Bones	
Spine	239
Tarsals and metatarsals	184
Carpals and metacarpals	109
Ribs	67
Tibia and fibula	49
Radius and ulna	48
Phalanges of fingers	38
Temporal bone	33
Phalanges of toes	31
Pelvis	27
Sternum	21
Femur	14
Humerus	10
Mandible	9
Scapula	8
Orbital margin	7
Parietal bone	5
Frontal bone	5
Maxilla	5
Sacrum	3
Zygoma	2
Patella	2
Clavicle	2
Occipital bone	1
Coccyx	1

Table 2: This table illustrates the location of tertiary syphilitic lesions by order of decreasing frequency (Roberts and Buikstra 2019, 368).

TABLE 11.7 Localization of 945 Tertiary Syphilitic Bone Lesions in Order of Decreasing Frequency

Bone	No.
Tibia	248
Nose and palate	238
Skull	179
Ulna	37
Ribs	35
Sternum	29
Clavicle	27
Metacarpals	21
Humerus	20
Radius	17
Femur	16
Mandible	14
Fibula	12
Spine	9
Nasal bone	9
Fingers	7
Pelvis bone	5
Metatarsals	4
Scapula	4
Ribs and sternum	3
Tarsals	3
Toes	3
Maxilla	3
Patella	1
Carpals	1

Source: After Fournier, 1906.

Figure 1: Complete skeletal remains for case #18-188.

Figure 2: This figure shows a circular pathology measuring 12.25 by 15.28 millimeters on the frontal bone near the coronal suture.

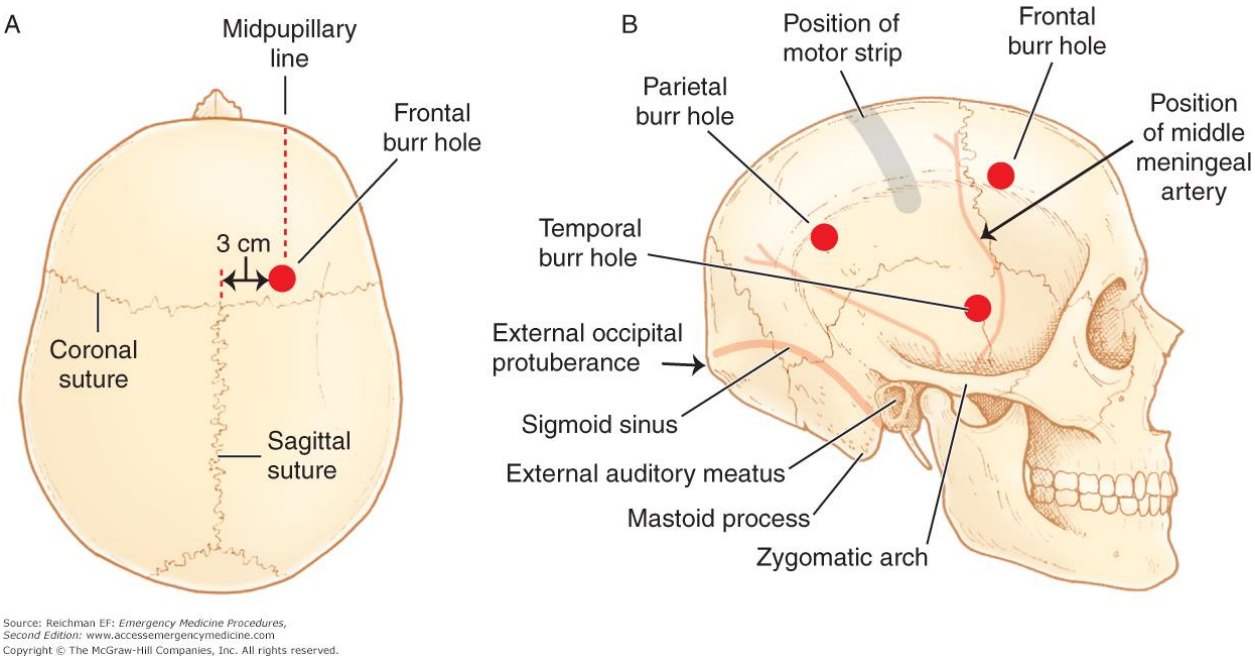

Figure 3: Illiterates the locations and size of burr hole trepanation.

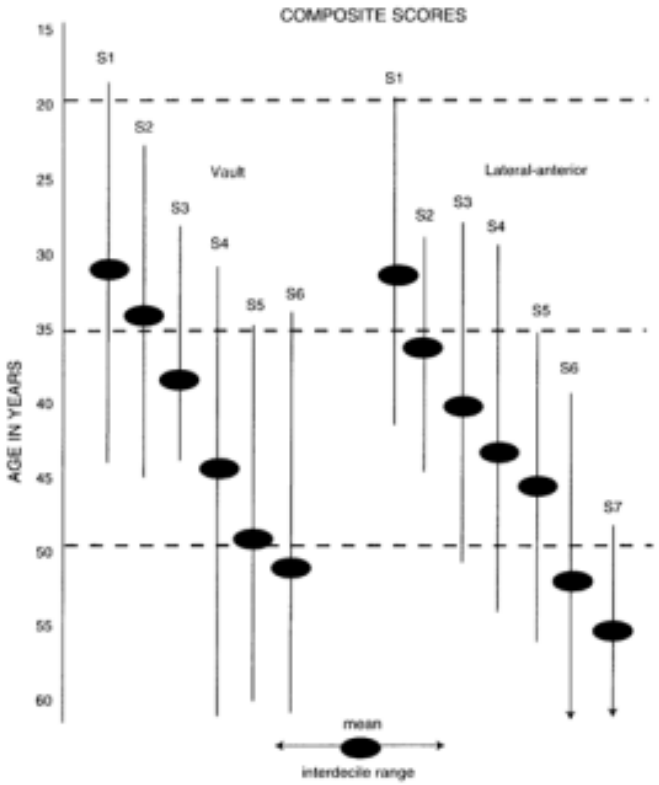

Figure 4: This figure illustrates how an "S" designation creates an overall age estimation.

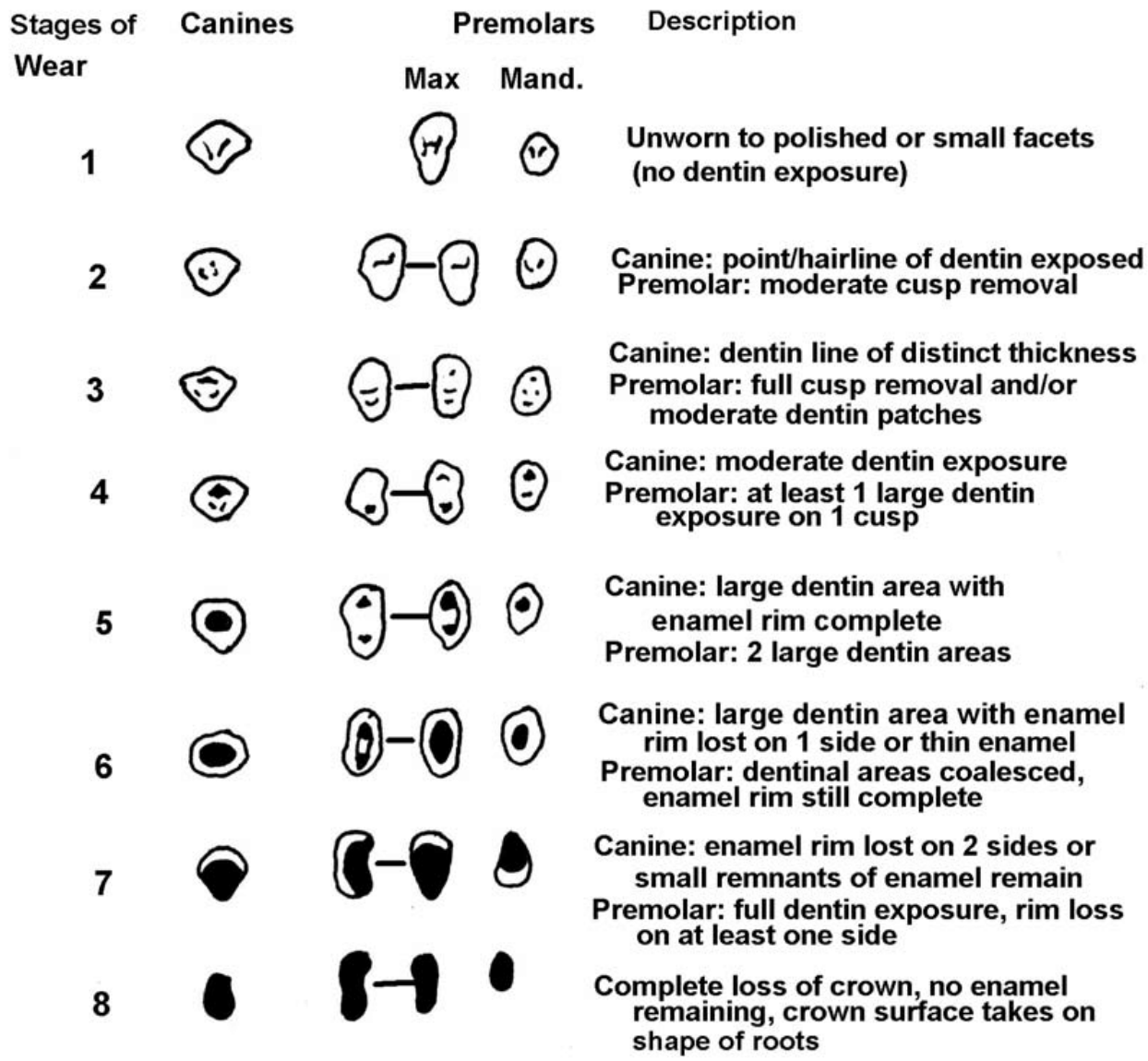

Figure 5: Surface wear scoring system for the incisors, canines and premolars (Scott, 1979).

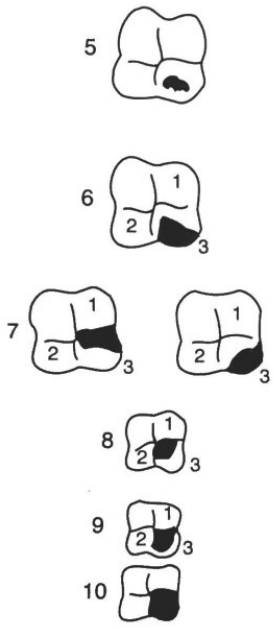

Score	Description
0	No information available (tooth not occluding, unerupted, antemortem or postmortem loss, etc.)
1	Wear facets invisible or very small
2	Wear facets large, but large cusps still present and surface features (crenulations, noncarious pits) very evident. It is possible to have pinprick size dentine exposures or dots which should be ignored. This is a quadrant with much enamel.
3	Any cusp in the quadrant area is rounded rather than being clearly defined as in 2. The cusp is becoming obliterated but is not yet worn flat.
4	Quadrant area is worn flat (horizontal) but there is no dentine exposure other than a possible pinprick sized dot.
5	Quadrant is flat, with dentine exposure one-fourth of quadrant or less. (Be careful not to confuse noncarious pits with dentine exposure.)
6	Dentine exposure greater: more than one-fourth of quadrant area is involved, but there is still much enamel present. If the quadrant is visualized as having three sides (as in the diagram) the dentine patch is still surrounded on all three sides by a ring of enamel.
7	Enamel is found on only two sides of the quadrant.
8	Enamel on only one side (usually outer rim) but the enamel is thick to medium on this edge.
9	Enamel on only one side as in 8, but the enamel is very thin—just a strip. Part of the edge may be worn through at one or more places.
10	No enamel on any part of quadrant—dentine exposure complete. Wear is extended below the cervicoenamel junction into the root.

Figure 26. Scott system for scoring surface wear in molars. Drawings by Zbigniew Jastrzebski (after Scott 1979: 214).

Figure 6: Surface wear scoring system for the molars (Scott, 1979).

Scores:

Sub-Pub Conc	Med Isch Pub Ram	Vent Arc
4	3	4

Linear Discriminant Functions (unpublished)

score	sex	prob M	prob F	accuracy	vars
-3.23	MALE	0.96	0.04	92 / 97	MV
-5.004	MALE	0.99	0.01	89 / 98	SMV
-6.376	MALE	1.00	0.00	88 / 98	SV
-4.072	MALE	0.98	0.02	87 / 96	SM

Logistic regression equation

2.526	**MALE**	**0.93**	**0.07**	98 / 74	SMV

Figure 7: This figure illustrates the results of the Klales (2012) method.

Sex estimation from Walker (2008)

Table 9. Logistic Regression Equations

Scores:

nuchal	mastoid	orbit	glabella	mental
4	4	2	3	4

Sex estimations:

score	sex	prob Male	prob F	accuracy	vars
-4.337	**MALE**	0.99	0.01	88 / 86	gl-ma-me
-3.106	**MALE**	0.96	0.04	85 / 83	gl-ma
-3.143	**MALE**	0.96	0.04	87 / 82	gl-me
-4.794	**MALE**	0.99	0.01	70 / 84	me-ma
-3.396	**MALE**	0.97	0.03	78 /78	or-me
-3.707	**MALE**	0.98	0.02	77 / 83	nu-ma

Figure 8: This figure illustrates the results of the Walker (2008) method.

Two Group Discriminant Function Results

Group	Classified into	Distance from	Probabilities Posterior	Typ F	Typ Chi	Typ R
WM	**WM**	78.9	0.991	0.089	0.000	0.026 (39/39)
BM		88.3	0.009	0.060	0.000	0.211 (16/19)

Figure 9: This figure is the result of the FORDISC 3.0 Two-Group Discriminant Functions Test for ancestry.

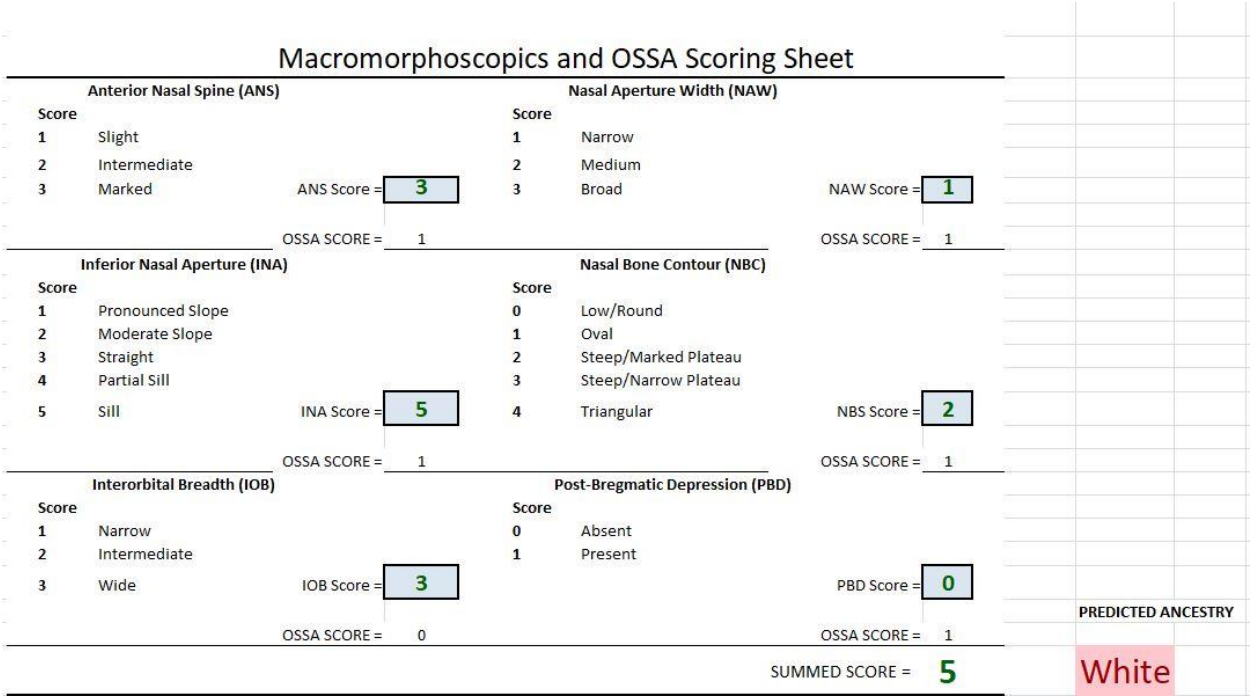

Macromorphoscopics and OSSA Scoring Sheet

Anterior Nasal Spine (ANS)

Score		
1	Slight	
2	Intermediate	
3	Marked	ANS Score = 3

OSSA SCORE = 1

Nasal Aperture Width (NAW)

Score		
1	Narrow	
2	Medium	
3	Broad	NAW Score = 1

OSSA SCORE = 1

Inferior Nasal Aperture (INA)

Score		
1	Pronounced Slope	
2	Moderate Slope	
3	Straight	
4	Partial Sill	
5	Sill	INA Score = 5

OSSA SCORE = 1

Nasal Bone Contour (NBC)

Score		
0	Low/Round	
1	Oval	
2	Steep/Marked Plateau	
3	Steep/Narrow Plateau	
4	Triangular	NBS Score = 2

OSSA SCORE = 1

Interorbital Breadth (IOB)

Score		
1	Narrow	
2	Intermediate	
3	Wide	IOB Score = 3

OSSA SCORE = 0

Post-Bregmatic Depression (PBD)

Score		
0	Absent	
1	Present	PBD Score = 0

OSSA SCORE = 1

SUMMED SCORE = 5

PREDICTED ANCESTRY

White

Figure 10: This figure illustrates the results of the Macromorphoscopics for ancestry.

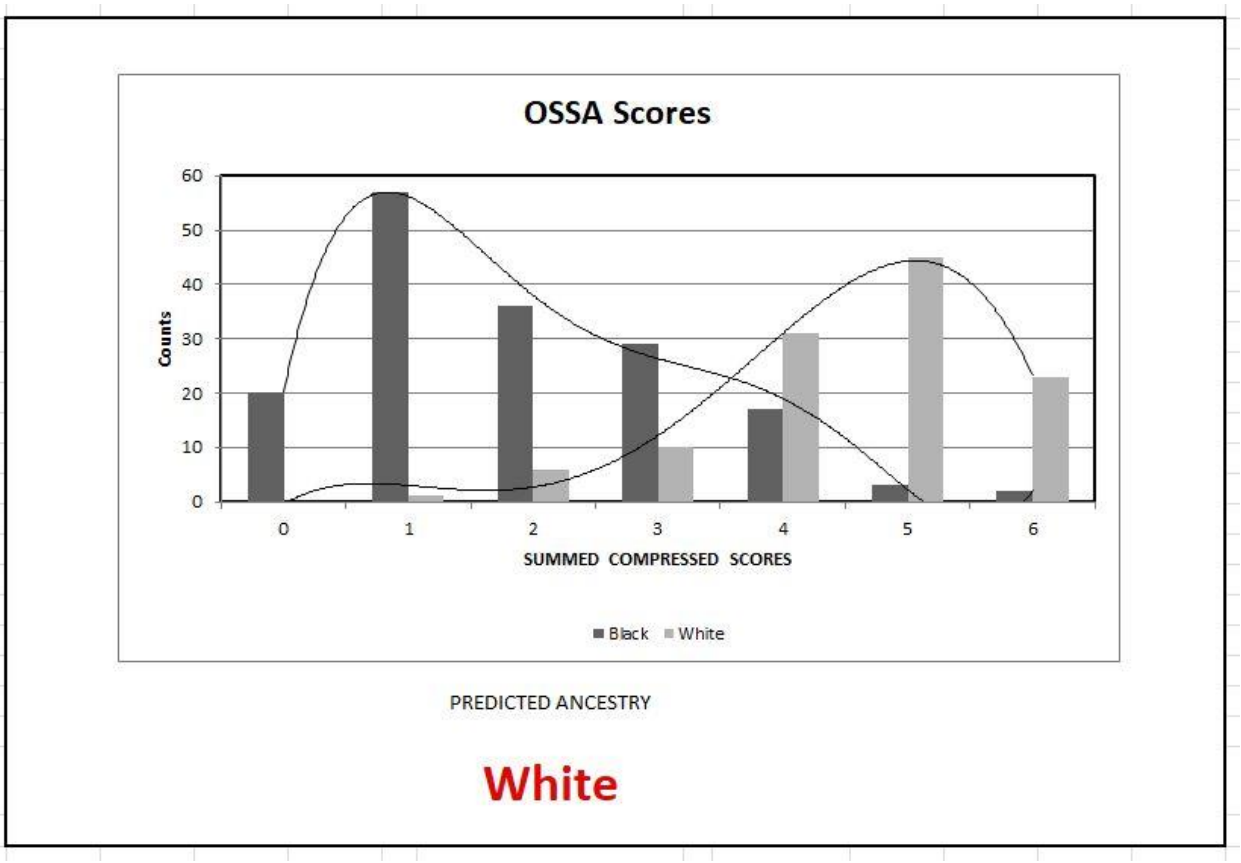

Figure 11: This figure illustrates the results of the OSSA scoring sheet for ancestry.

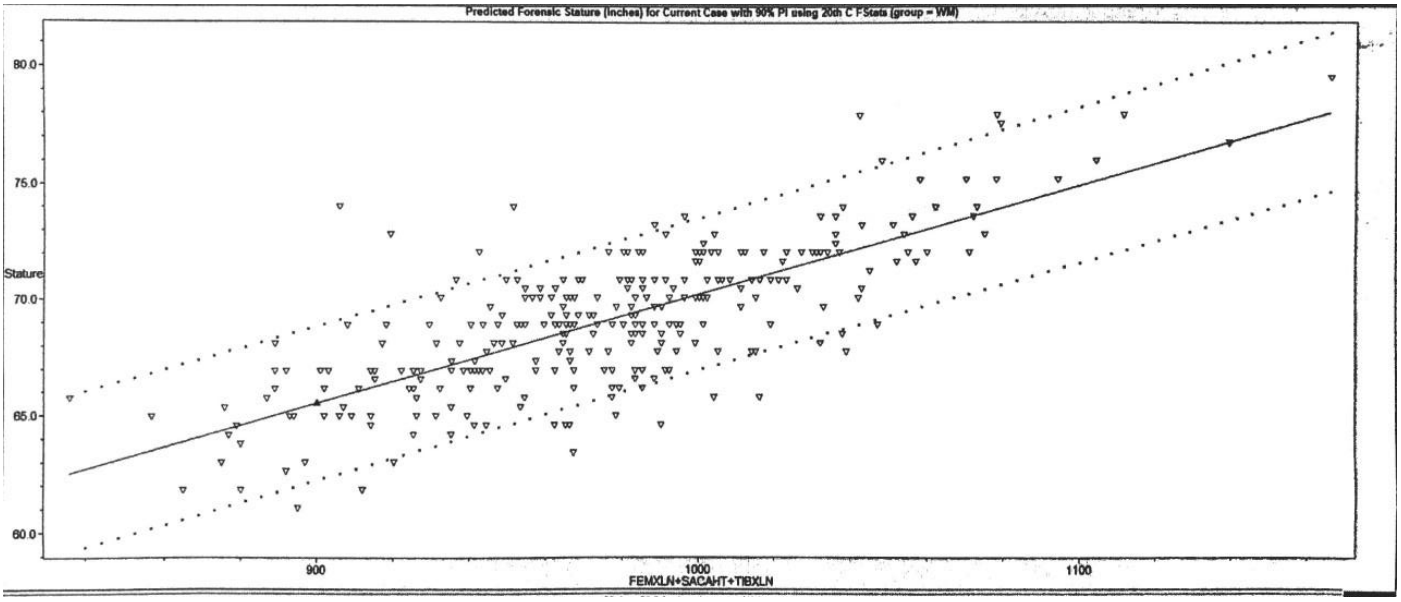

Figure 12: This figure illistrates the results of FORDISC 3.0 for stature.

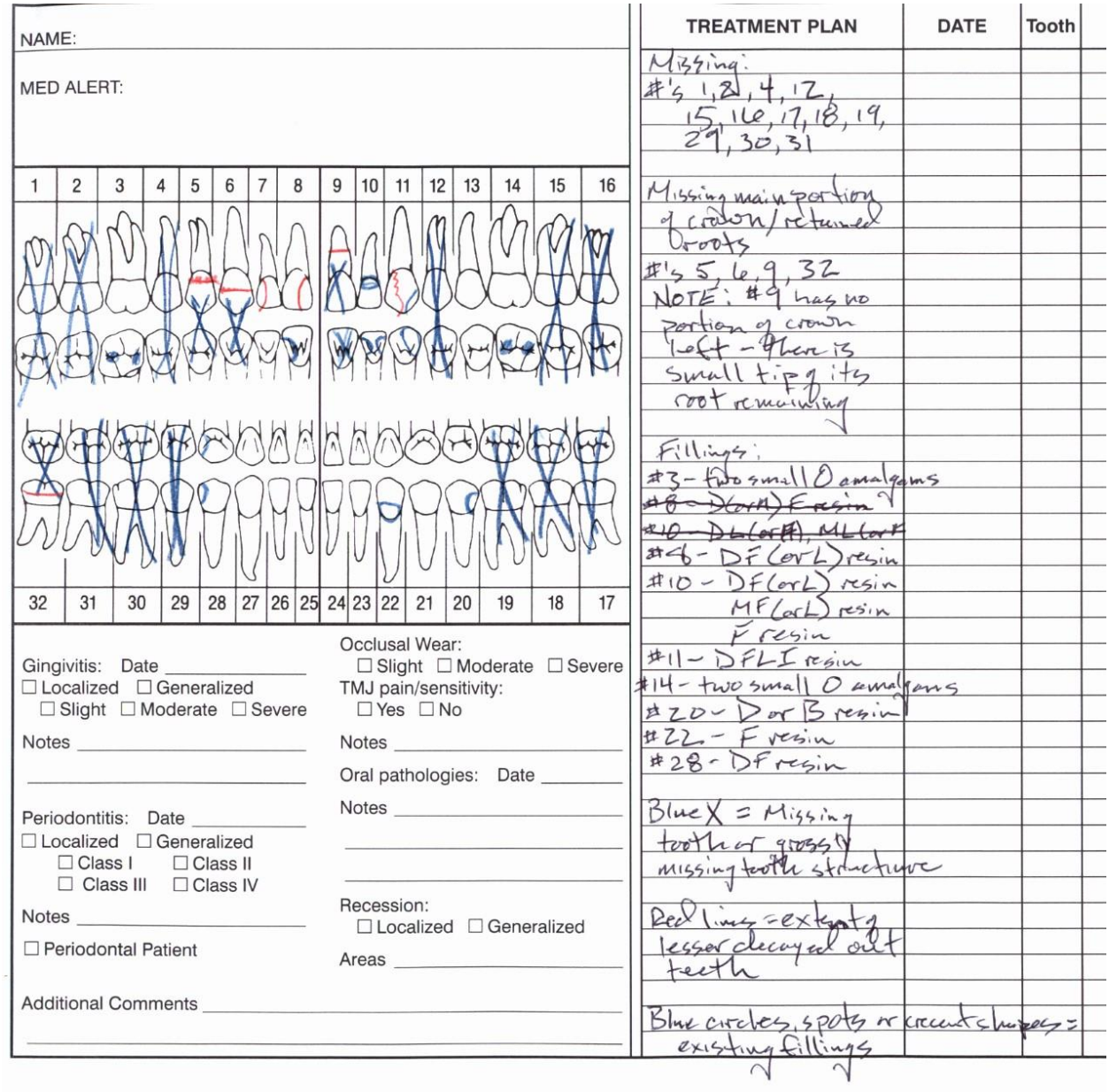

Figure 13: This figure illustrates the analysis of the dental x-rays from the Curry Health Center at the University of Montana.

Figure 14: This figure is a dental x-ray for LM^1 case #18-188.

Figure 15: This figure is a dental x-ray for the RP^2, RM^1 and a retained root for RM^2 of case #18-188.

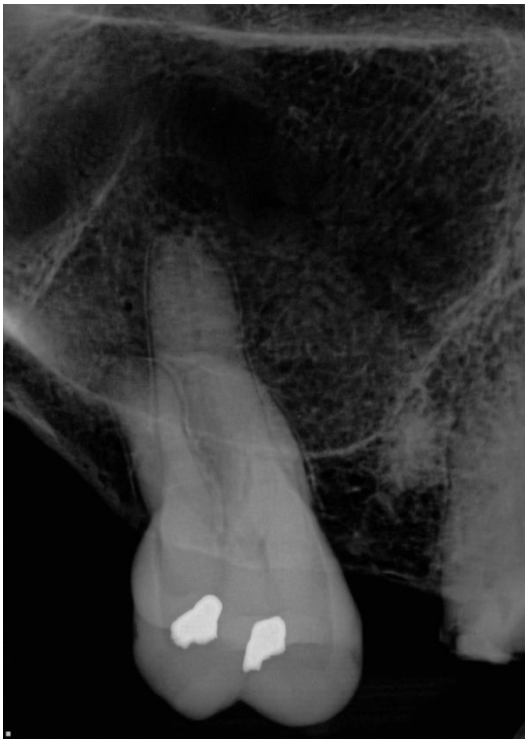

Figure 16: This figure is a dental x-ray for RM[1] for case #18-188.

Figure 17: This figure is a dental x-ray for RM[1] for case #18-188.

Figure 18: This figure is a dental x-ray for LP^2 and LM^2.

Figure 19: This figure is a dental x-ray for right maxillary central and lateral incisor.

Figure 20: This figure is a dental x-ray for LI^2 and LC^1 case #18-188.

Figure 21: This figure is a dental x-ray for RC_1 and RP_1 case #18-188.

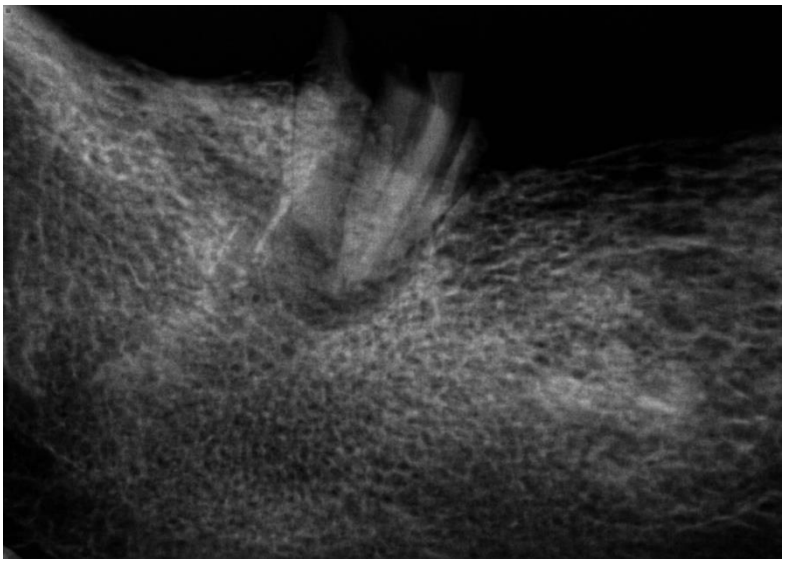

Figure 22: This figure is a dental x-ray for the right mandibular third molar.

Figure 23: This figure is a dental x-ray for case #18-188 mandibular incisors.

Figure 24: This figure is a dental x-ray for LC_1, LP_1 and LP_2 case #18-188.

Figure 25: This figure shows osteoporosis on the distal inferior side of the left clavicle.

Figure 26: This figure shows osteoporosis on the inferior side of the right clavicle.

Figure 27: This figure shows the osteoporosis on the anteroinferior side of the sacrum.

Figure 28: This figure shows osteoporosis on the posterosuperior left side of the sacrum.

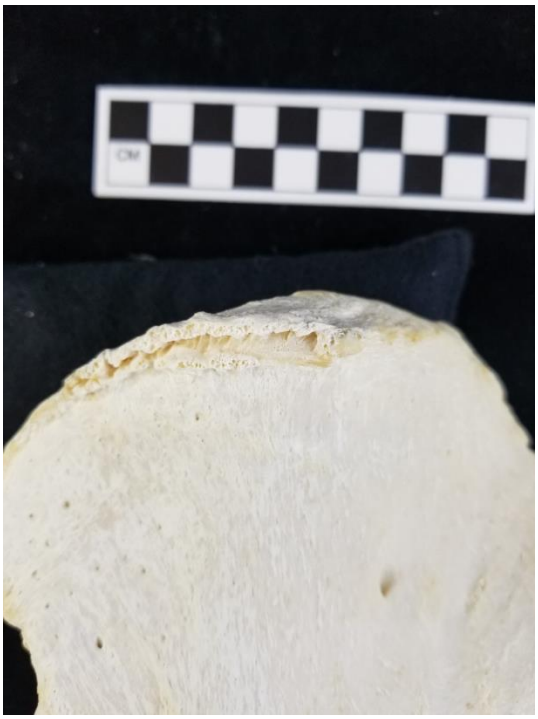

Figure 29: This figure shows osteophytes on the iliac crest of the left os coxae.

Figure 30: This figure shows osteophytes on the ischial tuberosity of the left os coxae.

Figure 31: This figure shows osteophytes on the preauricular surface of the right os coxae.

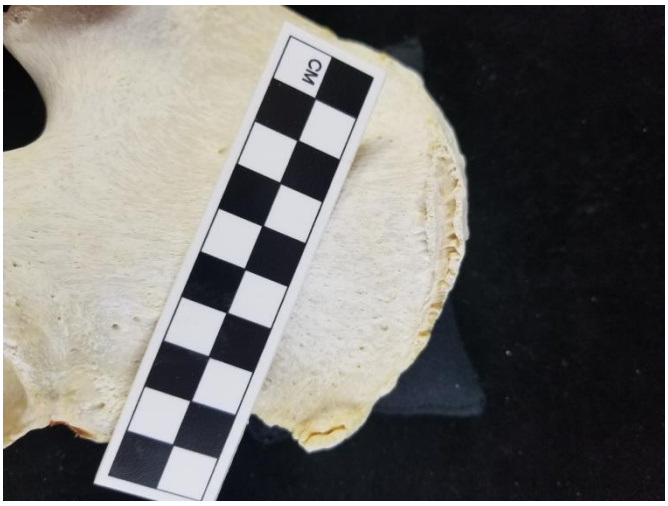

Figure 32: This figure shows osteophytes on the iliac crest of the right os coxae.

Figure 33: This figure shows osteophytes on the ischial tuberosity of the right os coxae.

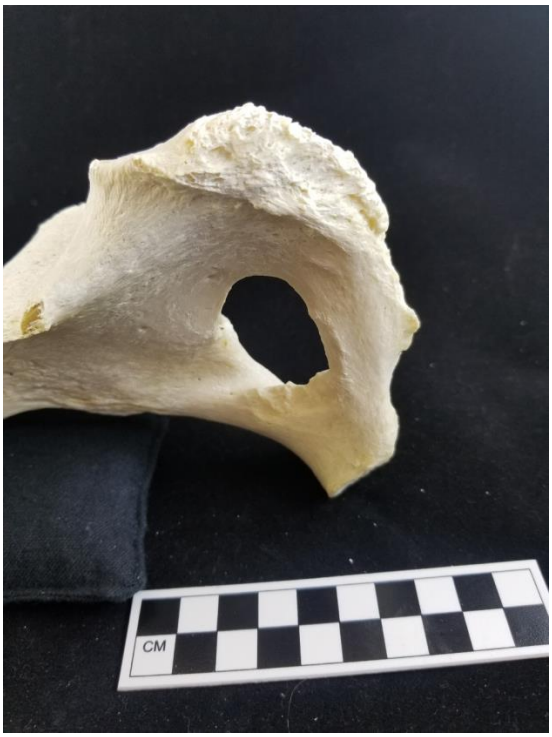

Figure 34: This figure shows osteoporosis on the ischial spine of the right os coxae.

Figure 35: This figure shows osteoporosis on the auricular surface of the right os coxae.

Figure 36: This figure shows an osteophyte on the spinal process of C-2.

Figure 37: This figure shows osteoporosis on C-3 and C-4.

Figure 38: This figure shows osteoporosis on T-4, T-5, T-6, T-7, T-8, T-9 and T-10.

Figure 39: This figure shows osteoporosis on T-4, T-5, T-6, T-7, T-8, T-9 and T-10.

Figure 40: This figure shows healed trauma to the left of the glabella and above the left eye orbit measuring 25.76 x 17.09 mm.

Figure 41: This figure shows a postmortem cut to the sternal end of the left clavicle.

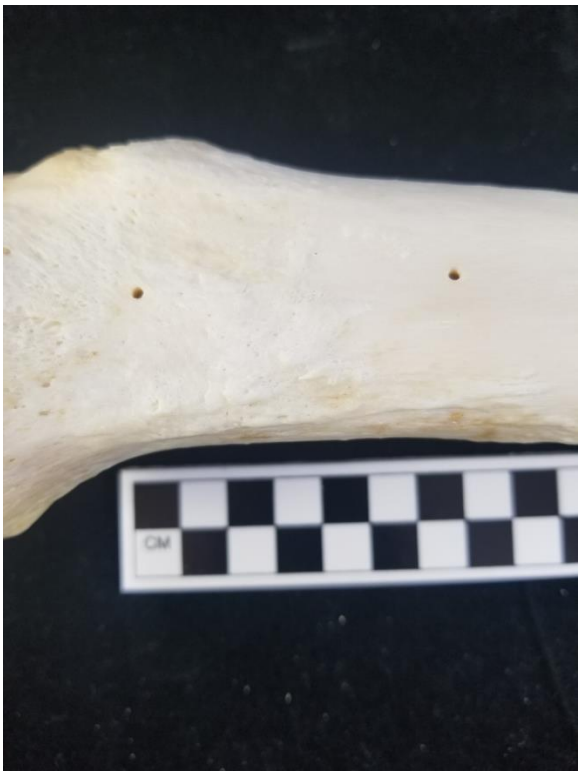

Figure 42: This figure shows postmortem drilling on the left tibia on the anterior proximal side measuring 41.75 mm apart.

References

Bass, W.M. (1995). *Human Osteology: A Laboratory and Field Manual* (3rd Ed.). Columbia, Missouri: Missouri Archaeological Society.

Brooks, S., and Suchey, J.M. (1990). Skeletal Age Determination Based on the Os Pubis: A Comparison of the Acsádi-Nemeskéri and Suchey-Brooks Methods. *Human Evolution*, 5(1): 227-238.

Buikstra, J. E., & Roberts, C. A. (2019). *Identification of pathological conditions in human skeletal remains* (3rd ed.). London: Elsevier Science.

Buikstra, J.E., and Ubelaker, D.H., editors. (1994). Standards: for Data Collection from Human Skeletal Remains. Fayetteville, AK: Arkansas Archeological Survey.

Genoves, S. (1959). L' estimation des differences sexuelles dans l' os coxal: Differences metriques et differences morphologiques. *Bulletins et Memoires Societe d' Anthropologie de Paris* 10: 3-95.

Gill, G. W. (1986). Craniofacial criteria in forensic race identification. In. K.J. Reichs (ed.) *Forensic Osteology: Advances in the Identification of Human Remains*. Pp. 143-159. Springfield. Illinois: C.C. Thomas.

Gross, C. G. (2012). *A hole in the head: more tales in the history of neuroscience*. Cambridge, MA: MIT Press.

Han, H.-J., Park, C.-W., Kim, E.-Y., Yoo, C.-J., Kim, Y.-B., & Kim, W.-K. (2009). One vs. Two Burr Hole Craniostomy in Surgical Treatment of Chronic Subdural Hematoma. *Journal of Korean Neurosurgical Society*, *46*(2), 87. doi: 10.3340/jkns.2009.46.2.87

Iscan, M.Y., and Loth, S.R. (1986). Estimation of age and determination of sex from the sternal rib. In: K.J. Reichs (ed.) *Forensic Osteology: Advances in the Identification of Human Remains*. Pp. 68-69. Springfield, Illinois: C.C. Thomas.

James, A. L., & Papsin, B. C. (2004). Device fixation and small incision access for pediatric cochlear implants. *International Journal of Pediatric Otorhinolaryngology*, *68*(8), 1017–1022. doi: 10.1016/j.ijporl.2004.03.007

Jantz, R. L., & Ousley, S. D. 2005. FORDISC 3.0: personal computer forensic discriminant functions. Knoxville, TN: University of Tennessee.

Klales, A.R., Ousley S.D., Vollner, J.M., 2012. A New Method of Sexing the Human Innominate Using Phenice's Nonmetric Traits and Statistical Methods. *American Journal of Physical Anthropology* 149:104-114.

Lovejoy, C.O., R.S. Meindl, R.P. Mensforth, and T.J. Barton, 1985. Multifactorial determination of skeletal age at death: A method and blind tests of its accuracy. Am. J. Phys, Anthrop. 68: 1-14.

Lovejoy, C. O., Meindl, R. S., Pryzbeck, T. R., and Mensdforth, R. P., (1985). Chronological metamorphosis of the auricular surface of the ilium: A new method for the determination of adult skeletal age at death. *American Journal of Physical Anthropology* 68: 15-28.

Ortner, D.J. (2003). Identification of Pathological Conditions in Human Skeletal Remains. (2nd Ed.). Amsterdam: Academic Press.

Phenice, T. W. (1969). A newly developed visual method of sexing in the os pubis. *American Journal of Physical Anthropology* 30: 297-301.

Rhine, S. (1990). Non-Metric skull racing. In. G.W. Gill and S. Rhine (eds.) Skeletal Attribution of Race: Methods for Forensic Anthropology. pp. 9-20. Albuquerque, New Mexico: Maxwell Museum of Anthropology, Anthropologic Papers Number 4.

Scott, E.C. 1979. Dental Wear Scoring Technique. *American Journal of Anthropology*. 51:213-218.

Todd, T.W. (1920). Age Changes in the Pubic Bone: I. The White Male Pubis. *American Journal of Physical Anthropology,* 3(1): 467-470.

Trotter, M., and Gleser, G. C. (1958). A re-evaluation of estimation of stature based on measurements of stature taken during life and of long bones after death. *American Journal of Physical Anthropology* 16: 79-123.

Trotter, M. (1970). Estimation of Stature From Intact Long Bones. In: T.D. Stewart (ed.) Personal Identification in Mass Disasters. Pp. 71 – 83. Washington, DC: Smithsonian Institution Press.

Walker PL. Sexing skulls using discriminant function analysis of visually assessed traits. American Journal of Physical Anthropology 2008;136(1):39–50.

White, T., Folkens P., 2005. The Human Bone Manual. Elsevier Academic Press, Burlington.